European Journal of Radiology Open 7 (2020) 100263

Contents lists available at ScienceDirect

European Journal of Radiology Open

journal homepage: www.elsevier.com/locate/ejro

Projected lung areas using dynamic X-ray (DXR)

Takuya Hino [a,*], Akinori Hata [a], Tomoyuki Hida [b], Yoshitake Yamada [c], Masako Ueyama [d], Tetsuro Araki [a], Takeshi Kamitani [b], Mizuki Nishino [a], Atsuko Kurosaki [e], Masahiro Jinzaki [c], Kousei Ishigami [b], Hiroshi Honda [b], Hiroto Hatabu [a], Shoji Kudoh [f]

[a] Center for Pulmonary Functional Imaging, Department of Radiology, Brigham and Women's Hospital, Harvard Medical School, 75 Francis St., Boston, MA, USA
[b] Department of Clinical Radiology, Graduate School of Medical Sciences, Kyushu University, 3-1-1 Maidashi, Higashi-ku, Fukuoka, Fukuoka, Japan
[c] Department of Diagnostic Radiology, Keio University School of Medicine, 35 Shinanomachi, Shinjuku-ku, Tokyo, Japan
[d] Department of Health Care, Fukujuji Hospital, Japan Anti-Tuberculosis Association, 3-1-24 Matsuyama, Kiyose, Tokyo, Japan
[e] Department of Diagnostic Radiology, Fukujuji Hospital, Japan Anti-Tuberculosis Association, 3-1-24 Matsuyama, Kiyose, Tokyo, Japan
[f] Japan Anti-Tuberculosis Association, 1-3-12 Kanda-Misakicho, Chiyoda-ku, Tokyo, Japan

ARTICLE INFO

Keywords:
dynamic X-ray
Chest radiograph
Pulmonary function
Health screening cohort
Projected lung area

ABSTRACT

Background: Dynamic X-ray (DXR) provides images of multiple phases of breath with less radiation exposure than CT. The exact images at end-inspiratory or end-expiratory phases can be chosen accurately.
Purpose: To investigate the correlation of the projected lung area (PLA) by dynamic chest X-ray with pulmonary functions.
Material and Methods: One hundred sixty-two healthy volunteers who received medical check-ups for health screening were included in this study. All subjects underwent DXR in both posteroanterior (PA) and lateral views and pulmonary function tests on the same day. All the volunteers took several tidal breaths before one forced breath as instructed. The outlines of lungs were contoured manually on the workstation with reference to the motion of diaphragm and the graph of pixel values. The PLAs were calculated automatically, and correlations with pulmonary functions and demographic data were analyzed statistically.
Results: The PLAs have correlation with physical characteristics, including height, weight and BMI, and pulmonary functions such as vital capacity (VC) and forced expiratory volume in one second (FEV_1). VC and FEV_1 revealed moderate correlation with the PLAs of PA view in forced inspiratory phase (VC: right, $r = 0.65$; left, $r = 0.69$. FEV1: right, $r = 0.54$; left, $r = 0.59$). Multivariate analysis showed that body mass index (BMI), sex and VC were considered independent correlation factors, respectively.
Conclusion: PLA showed statistically significant correlation with pulmonary functions. Our results indicate DXR has a possibility to serve as an alternate method for pulmonary function tests in subjects requiring contact inhibition including patients with suspected or confirmed covid-19.

1. Introduction

Pulmonary function tests (PFTs) provide the useful information about detection as well as characteristics or severity of lung disease. Forced vital capacity (FVC) have played an important role for the diagnosis of idiopathic pulmonary fibrosis (IPF) for many years. Patients can be diagnosed as interstitial lung disease if percent vital capacity (%VC) is lower than 80 %. It also correlates with a poor outcome in patient with IPF [1,2]. Forced expiratory volume in one second (FEV_1) is also an important predictor in PFTs, especially for screening of chronic obstructive pulmonary disease (COPD). Forced expiratory volume percent in one second divided by FVC (FEV_1/FVC, FEV_1%) is used for the

Abbreviation: BMI, body mass index; COPD, chronic obstructive pulmonary disease; DXR, dynamic X-ray; FPD, flat-panel detector; FEV1, forced expiratory volume in one second; FEV1%, forced expiratory volume percent in one second divided by FVC; FVC, forced vital capacity; IPF, idiopathic pulmonary fibrosis; %FEV1, percent predicted FEV1; %VC, percent vital capacity; PA, posteroanterior; PLA, projected lung area; PFTs, pulmonary function tests; TV, tidal volume; TLC, total lung capacity; VC, vital capacity.

* Corresponding author at: Center for Pulmonary Functional Imaging, Department of Radiology, Brigham and Women's Hospital and Harvard Medical School, 75 Francis Street, Boston, MA 02115, USA.
E-mail address: thino@bwh.harvard.edu (T. Hino).

https://doi.org/10.1016/j.ejro.2020.100263
Received 16 July 2020; Received in revised form 31 July 2020; Accepted 24 August 2020

diagnosis of COPD. The severity of COPD is classified with percent predicted FEV_1 (%FEV_1) [3,4]. Previous studies have reported that total lung capacity (TLC) had a good correlation with projected lung area (PLA) by chest radiograph [5–13]. Harris et al. [8] reported the simple way of predicting TLC with chest radiograph image of both posterior-anterior (PA) and lateral views. However, the correlation between PLA and pulmonary function has not been studied.

Recently, dynamic X-ray (DXR) with flat-panel detector (FPD) enabled to evaluate pulmonary functions such as blood flow and diaphragm motion [14–19]. CT also has the potential; however, chest radiograph is simpler and less expensive. DXR can provide images of multiple phases of breath with less radiation exposure than CT. Therefore, the exact images at end-inspiratory or end-expiratory phases can be chosen accurately.

The aim of this study is to investigate the correlation between PLA measured by DXR and pulmonary functions. If good correlations between PLA and PFTs are observed, it may provide the possibility of using DXR as an alternative method for assessing pulmonary functions in patients with contact inhibition such as suspected or confirmed covid-19 or other infectious lung diseases instead of PFTs.

2. Material and methods

2.1. Study population

This prospective study was approved by the ethics committee. One hundred and ninety-three volunteers who received medical checkups for health screening from May 2013 to February 2014 were enrolled in this study. The criteria for including this study were as follows; (a) 20 years of age or more; (b) no status of pregnancy, potential pregnancy, or lactating; (c) scheduled for conventional chest radiography; (d) undergoing PFTs. Thirty-one volunteers were excluded for the reasons as follows; incomplete dataset of chest radiography such as prominent image noise (n = 14), lack of examination in deep expiratory phase (n = 12), and lack of pulmonary function test or personal data (n = 5). Finally, a total of 162 volunteers were analyzed in this study.

2.2. Image protocol of dynamic X-ray

PA and lateral DXR was performed in the standing position using a prototype X-ray system (Konica Minolta Inc., Tokyo, Japan) composed of an FPD (PaxScan 4030CB, Varian Medical Systems Inc., Salt Lake City, UT, USA) and a pulsed X-ray generator (DHF-155HII with Cineradiography option, Hitachi Medical Corporation, Tokyo, Japan). During the examination, all the participants took several tidal breaths before one forced breath. Conditions for DXR were the same as the previous reports [16–19]: tube voltage, 100 kV; tube current, 50 mA; pulse duration of pulsed X-ray, 1.6 ms; source-to-image distance, 2 m; additional filter, 0.5 mm Al +0.1 mm Cu. The additional filter was used to filter out soft X-rays. The exposure time was approximately 10–15 s. The pixel size was 388 × 388 μm, the matrix size was 1024 × 768, and the overall image area was 40 × 30 cm. The dynamic image data, captured at 15 frames/s, were synchronized with the pulsed X-ray, which prevented excessive radiation exposure to the subjects. The entrance surface dose was approximately 0.3–1.0 mGy.

2.3. Image analysis

The data of DXR were assessed using prototype software (Konica Minolta Inc., Tokyo, Japan) installed in an independent workstation (Operating system: Windows 7 Professional 64-bit Service Pack 1; Microsoft, Redmond WA; CPU: Intel® CoreTM i5-6500, 3.20 GHz; random access memory, 16 GB). With reference to the motion of diaphragm and the graph of pixel value, the outline of the lung of both posteroanterior and lateral view was contoured manually by radiologist with seven-year experience (T.H.). The slope of pixel value frequently inversed in the transition between inspiration and expiration due to the change of lung volume as had been reported in the previous study [20]. PLA was calculated automatically by the software. PLA in both forced inspiratory and expiratory phase was measured in 162 volunteers. PLAs in both tidal inspiratory and expiratory phase was also measured with the same method in 90 volunteers. Several phases of images were gathered in tidal breathing, so the average of PLA was calculated. When the borders of lungs were ambiguous, the outer border was defined as right one in accordance with the magnification effect of lateral image. Representative cases are shown on Figs. 1–5, which include PLA curve during respiration. Note the resemblance of PLA curve over frame with those from spirometry. There was an impression that older subjects had larger tidal volume. In this study, several cases with decreased pulmonary function confirmed by PFTs were also shown in Figs. 6 and 7.

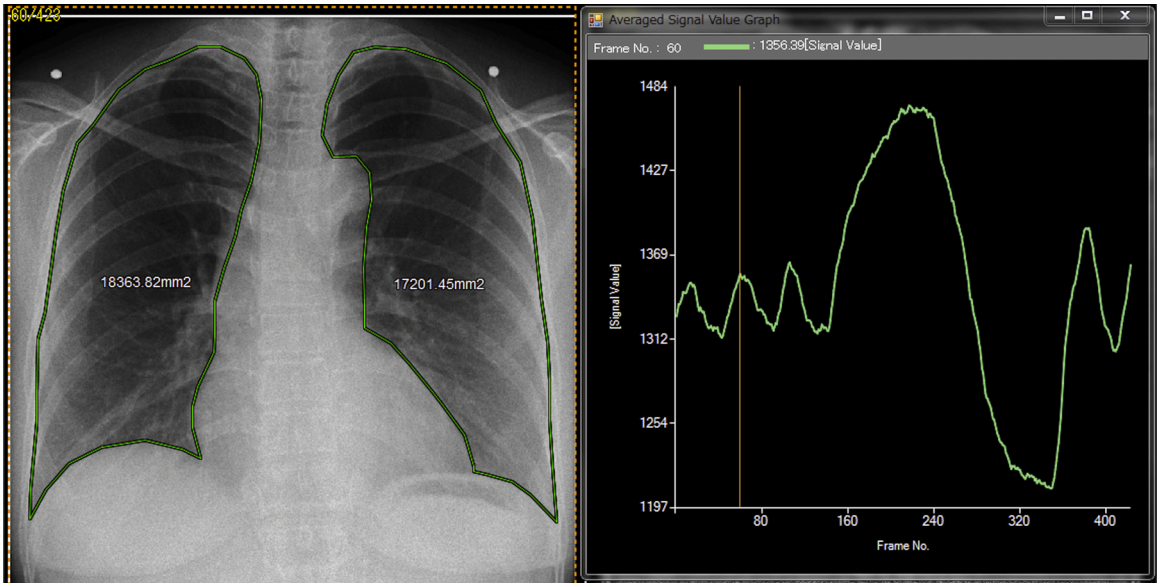

Fig. 1. Projected Lung Area (PLA) of right and left lungs in PA projection.
53-year-old woman with no smoking history. Projected Lung Area (PLA) of right and left lungs in PA projection in the tidal end-inspiratory phase are shown. The graph on the right represents averaged signal value of the image. Measurement was performed manually with reference to the graph and diaphragm motion.

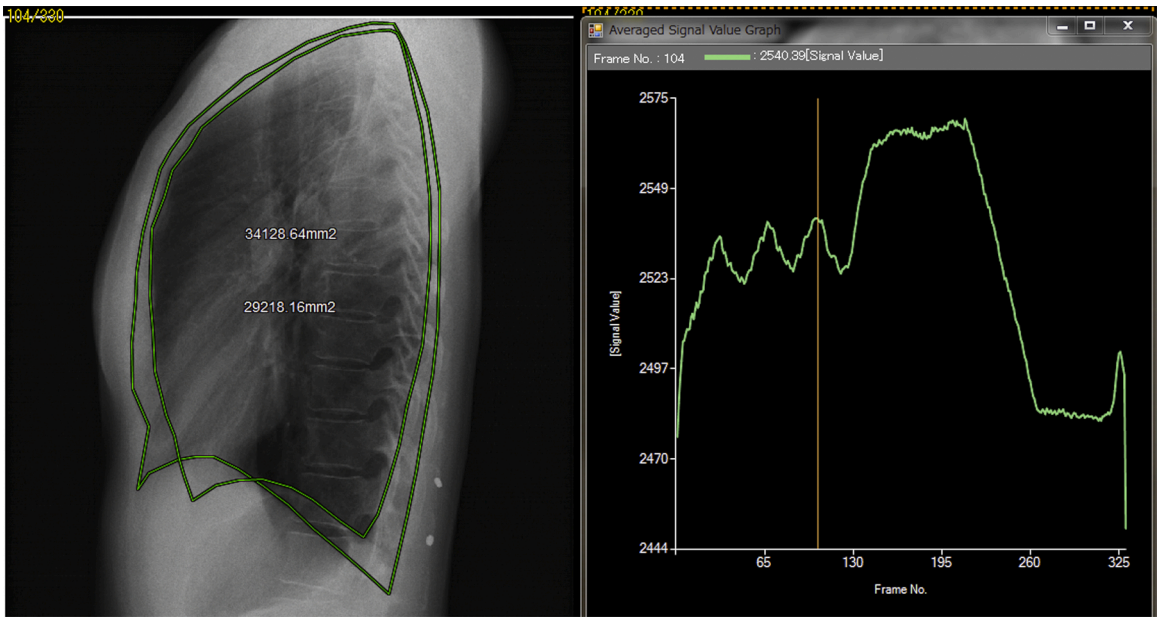

Fig. 2. Projected Lung Area (PLA) of right and left lungs in the left lateral projection.
55-year-old woman with no smoking history. PLA in the left lateral projection in the tidal end-inspiratory phase. The graph on the right represents averaged signal value of the image. Measurement was performed manually with reference to the graph and diaphragm motion.

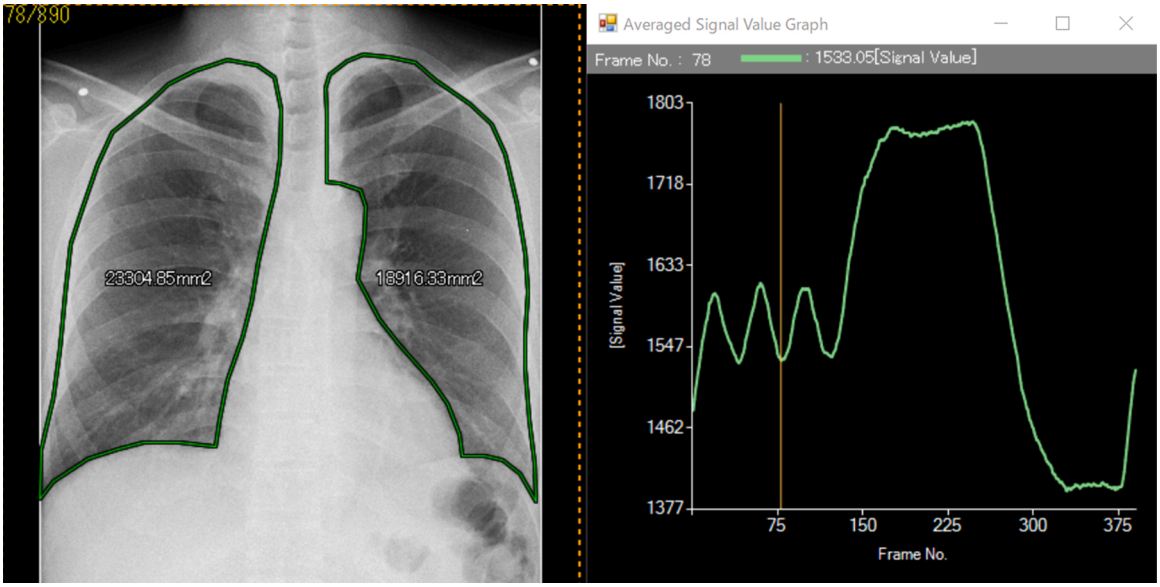

Fig. 3. Projected Lung Area (PLA) of right and left lungs in PA projection.
38-year-old man with smoking history: 17 pack-years. PLA in PA projection in the tidal end-expiratory phase. The graph on the right represents averaged signal value of the image. Measurement was performed manually with reference to the graph and diaphragm motion.

2.4. Pulmonary function tests (PFTs)

All volunteers underwent PFTs on the same day of DXR. Parameters of PFTs were decided according to the guideline of American Thoracic Society [21] using a pulmonary function instrument with computer processing (DISCOM-21 FX, Chest MI Co, Tokyo, Japan). The information of pulmonary functions was obtained as follows: tidal volume (TV), vital capacity (VC), vital capacity as percent of predicted % (%VC), forced expiratory volume in 1 s (FEV_1), forced expiratory volume % in 1 s (FEV_1%), percent predicted forced expiratory volume in one second ($\%FEV_1$) and the maximum flow rate at 25 % of forced VC divided by body height (V25/Ht).

2.5. Statistical analysis

Measured numeric value was described as follows: mean value ± -standard deviation. The PLAs of both PA and lateral views in forced inspiratory phase (PLA-INS-PA, PLA-INS-LAT), that in forced expiratory phase (PLA-EX-PA, PLA-EX-LAT), that in tidal inspiratory phase (PLA-ins-PA, PLA-ins-LAT) and that in tidal expiratory phase (PLA-ex-PA,

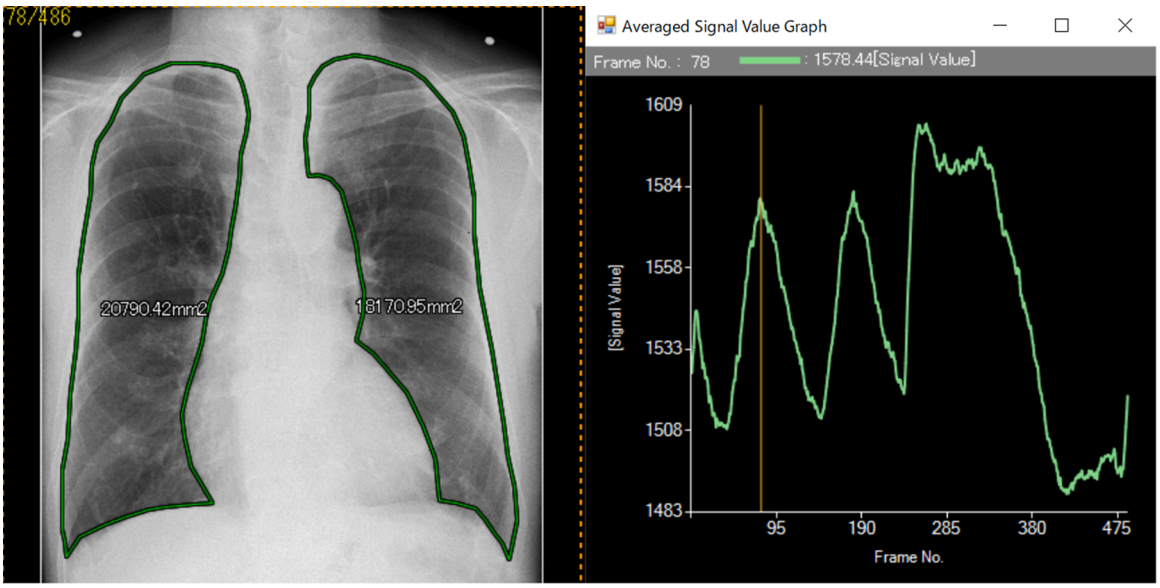

Fig. 4. Projected Lung Area (PLA) of right and left lungs in PA projection.
93-year-old man with smoking history: 40 pack-years. PLA in PA projection in the tidal end-inspiratory phase. The graph on the right represents averaged signal value of the image. Measurement was performed manually with reference to the graph and diaphragm motion.

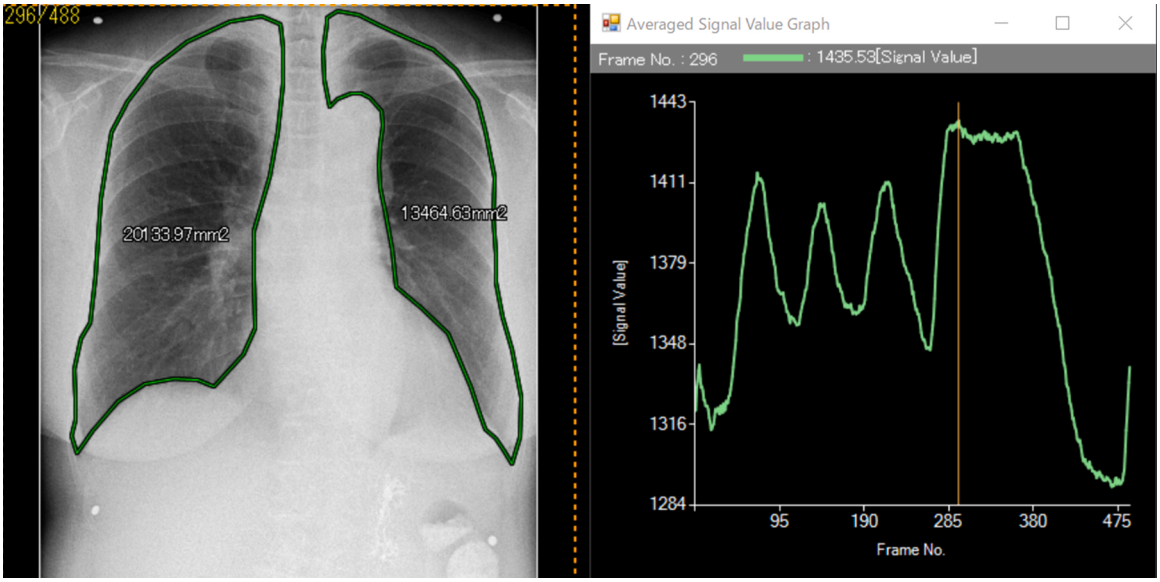

Fig. 5. Projected Lung Area (PLA) of right and left lungs in PA projection.
79-year-old woman with no smoking history. PLA in PA projection in the forced end-inspiratory phase. The graph on the right represents averaged signal value of the image. Measurement was performed manually with reference to the graph and diaphragm motion.

PLA-ex-LAT) was measured. The difference of PLA between the right and left lung was evaluated with paired t-test. The correlation between PLA and each demographic data including pulmonary functions, height, weight, body mass index (BMI), sex, pack-year was assessed with Spearman's rank correlation coefficient. Several items with statistical significance in univariate analysis were assessed with multiple linear regression analysis.

Statistical analyses were conducted with EZR (Saitama Medical Center, Jichi Medical University, Saitama, Japan), a graphical user interface for R 2.13.0 (R Foundation for Statistical Computing, Vienna, Austria) [22,23]. More precisely, it is a modified version of R commander designed to add statistical functions frequently used in biostatistics. A two-sided P values of less than 0.05 were considered statistically significant.

3. Results

3.1. Demographic data and the PLA

Demographic characteristics and pulmonary function are shown in Table 1. In this study, %VC was lower than 80 % in three subjects and FEV_1% was lower than 70 % in six subjects. No significant change is observed between the dataset of all the volunteers and that of ninety volunteers with PLA of both forced and rest breathing. The right PLA

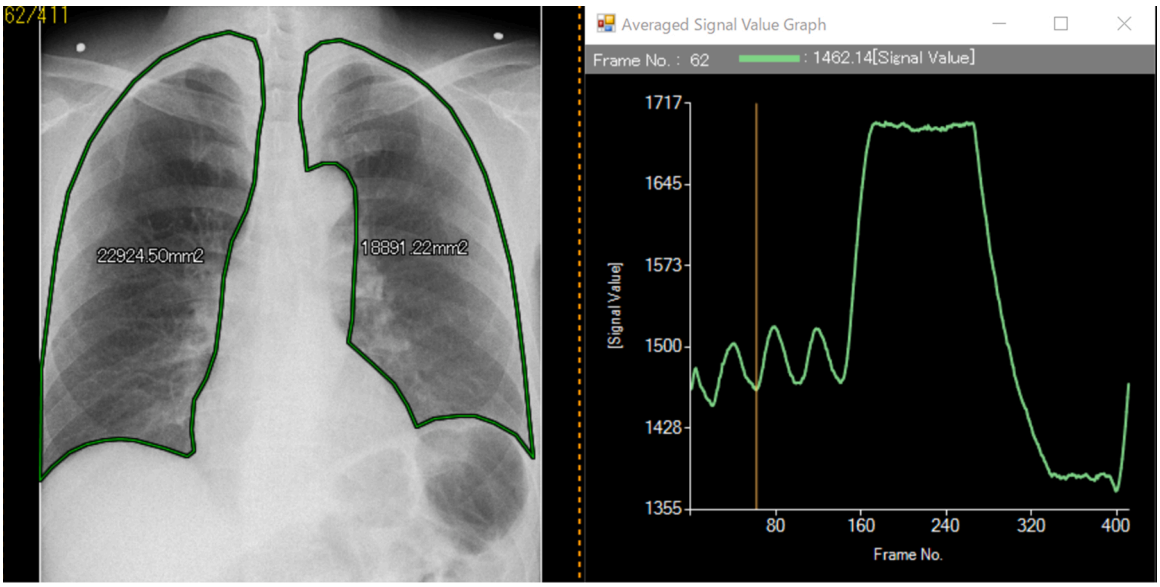

Fig. 6. Projected Lung Area (PLA) of right and left lungs in PA projection.
57-year-old man with smoking history: 37 pack-years. Pulmonary function test showed decreased forced expiratory volume percent (57.3 %) in one second (FEV1.0 %); obstructive pulmonary disorder was suspected. PLA in PA projection in the tidal end-expiratory phase. The graph on the right represents averaged signal value of the image. Measurement was performed manually with reference to the graph and diaphragm motion.

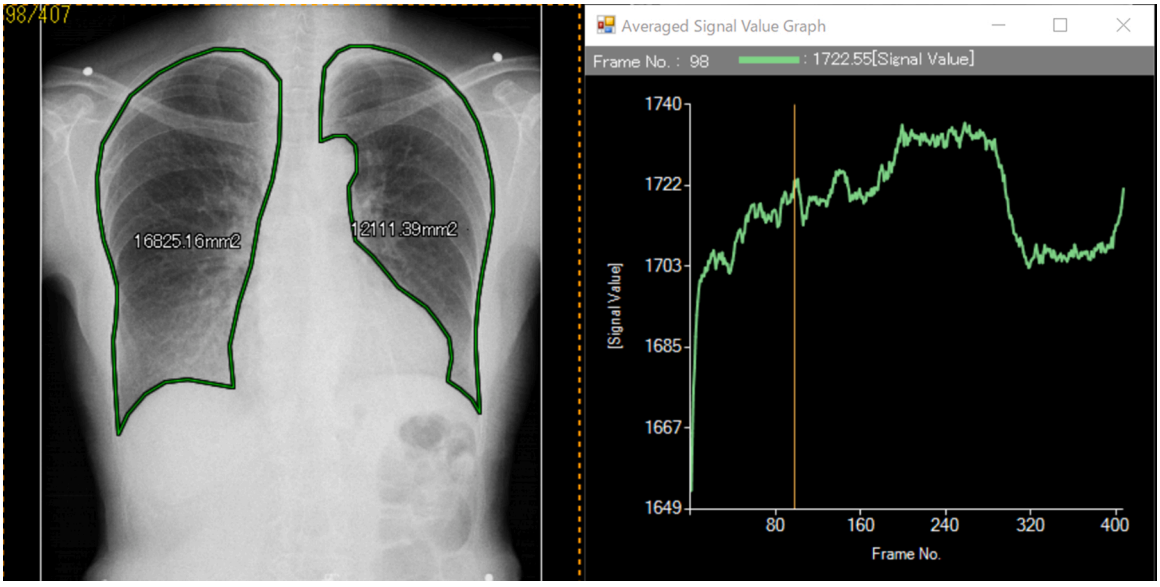

Fig. 7. Projected Lung Area (PLA) of right and left lungs in PA projection.
81-year-old man with no smoking history. Pulmonary function test showed decreased vital capacity (62.9 %) as percent of predicted (%VC); restrictive pulmonary disorder was suspected. PLA in PA projection in the tidal end-expiratory phase. The graph on the right represents averaged signal value of the image, which showed the disorder of curve. Measurement was performed manually with reference to the graph and diaphragm motion.

was larger than that of the left lung in both PA and lateral view images of each phase with statistical significance (Table 2).

3.2. Association between the PLA and demographic data or pulmonary function

Table 3 showed the result of univariate analysis between the PLA of PA image and each parameter including pulmonary function and personal data. The PLA of PA image presented moderate correlation with height, sex, VC and FEV_1, BMI and V25/Ht. There was a tendency that the numeric values of correlation coefficient were higher in forced breathing. The mild correlation between PLA and tidal volume (TV) was observed only in forced inspiratory phase. The mild correlation between PLA and pack/year was observed only in forced breathing. No significant correlation between PLA and FEV_1% or %FEV_1 was observed.

The PLA in lateral image demonstrated the different results as shown

Table 1
Age, Sex, Height, Weight, BMI, Smoking History, and pulmonary functions.

	All volunteers (n = 162)		Volunteers with PLA in both forced and tidal phase (n = 90)	
Variables	Mean ± SD [range] or n (%)		Mean ± SD [range] or n (%)	
Age (years)	56.8 ± 10.3	[36–93]	57.0 ± 11.0	[36–90]
Sex				
Female	69	−42.60%	43	−47.80%
Male	93	−57.40%	47	−52.20%
Height (cm)	163.4 ± 9.0	[137.9–184.2]	162.6 ± 9.2	[137.9–183.7]
Weight (kg)	60.2 ± 10.8	[35.0–98.4]	59.7 ± 10.7	[37.0–98.4]
BMI (kg/m^2)	22.4 ± 2.8	[15.1–34.2]	22.5 ± 2.9	[15.1–34.2]
Smoking History				
Never	91	−56.20%	61	−67.80%
Current or former	71	−43.80%	29	−32.20%
Pack/year	10.8 ± 16.9	[0–76]	7.9 ± 15.5	[0–76]
Pulmonary Functions				
TV (L)	0.75 ± 0.36	[0.22–2.30]	0.78 ± 0.40	[0.22–2.30]
VC (L)	3.41 ± 0.80	[1.24–5.69]	3.36 ± 0.86	[1.24–5.69]
%VC	108.6 ± 14.5	[62.9–159.6]	109.2 ± 15.9	[62.9–159.6]
FEV_1 (L)	2.70 ± 0.65	[1.06–4.72]	2.67 ± 0.70	[1.06–4.72]
FEV_1%	80.9 ± 6.3	[57.3–97.3]	80.8 ± 6.7	[57.3–97.3]
%FEV_1	105.3 ± 14.0	[61.7–163.9]	106.2 ± 14.5	[72.1–163.9]
V25/Ht (L/sec/m)	0.66 ± 0.31	[0.16–1.97]	0.65 ± 0.34	[0.16–1.97]

BMI, body mass index; FEV1, forced expiratory volume in one second; FEV1%, forced expiratory volume percent in one second divided by forced vital capacity; %FEV1, percent predicted FEV1; %VC; percent vital capacity; PLA, projected lung area; SD, standard deviation; TV, tidal volume; V25/ht, the maximum flow rate at 25 % of forced VC divided by body height; VC, vital capacity.

Table 2
Projected areas of the right and left lungs on PA and RL projections during forced breathing and tidal breathing.

PLA	Right lung Mean ± SD [range]	Left lung Mean ± SD [range]	p value
Forced breathing (n = 162)			
PLA-INS-PA (cm^2)	241.3 ± 29.5 [129.0–325.9]	200.6 ± 31.5 [86.6–277.8]	<0.001
PLA-EX-PA (cm^2)	173.1 ± 30.0 [91.3–246.7]	141.3 ± 26.7 [61.3–216.7]	<0.001
PLA-INS-LAT (cm^2)	434.5 ± 60.3 [253.3–591.1]	398.2 ± 54.7 [266.2–534.4]	<0.001
PLA-EX-LAT (cm^2)	286.4 ± 51.6 [162.4–431.3]	269.7 ± 43.8 [173.8–401.8]	<0.001
Tidal breathing (n = 90)			
PLA-ins-PA (cm^2)	211.6 ± 31.4 [111.9–281.2]	172.0 ± 30.7 [77.6–253.9]	<0.001
PLA-ex-PA (cm^2)	197.4 ± 31.4 [108.7–268.8]	160.3 ± 28.9 [73.8–229.1]	<0.001
PLA-ins-LAT (cm^2)	365.9 ± 55.1 [217.5–488.9]	329.3 ± 48.4 [231.4–454.1]	<0.001
PLA-ex-LAT (cm^2)	332.9 ± 55.2 [191.6–461.2]	300.1 ± 48.2 [204.2–433.5]	<0.001

PLA, projected lung area; PLA-INS-PA, PLA of PA view in forced inspiratory phase; PLA-EX-PA, PLA of PA view in forced expiratory phase; PLA-INS-LAT, PLA of lateral view in forced inspiratory phase; PLA-EX-LAT, PLA of lateral view in forced expiratory phase; PLA-ins-PA, PLA of PA view in tidal inspiratory phase; PLA-ex-PA, PLA of PA view in tidal expiratory phase; PLA-ins-LAT, PLA of lateral view in tidal inspiratory phase; PLA-ex-LAT, PLA of lateral view in tidal expiratory phase; SD, standard deviation.

in Table 4. Height, weight and sex had mild to moderate correlations with the PLA in each respiratory phase. TV showed mild correlation with the PLA in inspiratory phase, which were a little higher than that in PA view. VC and FEV_1 revealed moderate correlation with the PLA of PA views in forced inspiratory phase. They also indicated mild correlation with that in other respiratory phase or lateral views. FEV_1% showed mild negative correlation with the PLA in inspiratory phase, which had no significant correlation with that in PA view.

We performed multivariate analysis to identify independent factors. Three factors: BMI, sex and VC, which had statistical significance in univariate analysis, and age were adopted and used. The detailed result is shown in Table 5. In PA view images, the PLA had statistically significant correlations with BMI and VC. In lateral view images, higher VC or age were statistically associated with larger PLA. Otherwise, statistically significant correlation with sex, and BMI was observed under the certain conditions.

4. Discussion

Several studies have shown that PLAs measured by chest radiograph had good correlation with TLC. Barnhard et al. divided lung images into ellipsoid components and estimated the lung volume with multiple diameters obtained by chest radiograph [5]. This method was modified by Loyd [6], in which multiple of PLAs by both PA and lateral views had good correlation with TLC [3,4]. These studies have been re-examined and improved for many years [5–9]. Some studies reported that CT image was also useful for the measurement of TLC in infants or children [11,13]. VC is calculated by TLC minus residual volume, thus VC and TLC correlate with each other. If VC and PLA have correlation with each other, there is a possibility that pulmonary functions have correlations with PLA measured by DXR. These findings indicate the possibility of using DXR instead of spirometry in subjects with whom close contact or use of mouth-piece is prohibited.

The PLAs of the left lung were smaller than those of the right lung. In PA view, the left PLA exclude the area overlapping cardiac shadow in accordance with the prior studies of planimetry [6,13,25]. Previous study reported that about 30 % of lung volume overlaps with shadows of diaphragm, heart and mediastinum by comparison with chest CT [24]. This fact might affect the PLAs measured in this study. In lateral views, flat panel detector was located along left side chest. It is also the reason why the left lung is smaller in volume compared to the right lung, when measured by DXR.

In univariate analysis, height, weight and sex showed significant correlation with PLA in each view. VC presented significant correlation with the PLAs as TLC did. These results indicate that the size of physique is associated with them. As for FEV_1, we have to keep in mind that it had significant correlation with VC ($r = 0.94$, $p < 0.001$). BMI, which is calculated by weight divided by square of height, showed no significance in some views. This was probably due to the cancellation by division. The same theory may be true of relative values such as %VC, FEV_1%, %FEV_1, and V25/Ht. The fact is equally important that the PLAs in inspiratory phase in PA image showed correlation with %VC and that in tidal breathing in lateral image with FEV_1%. TV also showed mild correlation with the PLA of lateral image in tidal breathing, but not that of PA image. In lateral image in tidal breathing, the curve and motion of diaphragm is visualized more clearly. This may be an important factor. Some autopsy study reported that smoking lead to the degeneration or

Table 3
Association of PLA of PA image with each parameter by Spearman's rank correlation.

	Right		Left		Right		Left	
	Spearman's rank correlation coefficient [95 %RI]	P value	Spearman's rank correlation coefficient [95 %RI]	P value	Spearman's rank correlation coefficient [95 %RI]	P value	Spearman's rank correlation coefficient [95 %RI]	P value
Variables	PLA-INS-PA				PLA-ins-PA			
Age	−0.13 [-0.29, 0.02]	0.08	−0.14 [-0.29, 0.02]	0.084	−0.20 [-0.39, 0.01]	0.058	−0.02 [-0.35, 0.06]	0.151
Height	0.70 [0.60, 0.77]	<0.001**	0.66 [0.56, 0.74]	<0.001**	0.65 [0.51, 0.76]	<0.001**	0.67 [0.54, 0.78]	<0.001**
Weight	0.33 [0.19, 0.47]	<0.001**	0.34 [0.20, 0.47]	<0.001**	0.22 [0.003, 0.41]	0.041*	0.24 [0.02, 0.43]	0.025*
BMI	−0.14 [-0.29, 0.02]	0.81	−0.11 [-0.27, 0.04]	0.15	−0.29 [-0.47, -0.08]	0.006**	−0.28 [-0.47, -0.07]	0.007**
Sex	0.54 [0.42, 0.65]	<0.001**	0.52 [0.39, 0.62]	<0.001**	0.39 [0.20, 0.56]	<0.001**	0.45 [0.26, 0.60]	<0.001**
Pack/ year	0.17 [0.02, 0.32]	0.023*	0.16 [-0.001, 0.31]	0.045*	0.10 [-0.11, 0.31]	0.34	0.10 [-0.11, 0.31]	0.33
TV	0.18 [0.02, 0.33]	0.021*	0.17 [0.01, 0.32]	0.029*	0.20 [-0.01, 0.40]	0.057	0.16 [-0.06, 0.36]	0.14
VC	0.68 [0.59, 0.76]	<0.001**	0.68 [0.59, 0.76]	<0.001**	0.56 [0.39, 0.69]	<0.001**	0.61 [0.45, 0.73]	<0.001**
%VC	0.26 [0.10, 0.40]	<0.001**	0.28 [0.13, 0.42]	<0.001**	0.24 [0.03, 0.43]	0.022*	0.28 [0.08, 0.47]	0.007**
FEV_1	0.59 [0.48, 0.69]	<0.001**	0.62 [0.51, 0.71]	<0.001**	0.51 [0.34, 0.66]	<0.001**	0.57 [0.40, 0.70]	<0.001**
FEV_1%	−0.15 [-0.30, 0.01]	0.062	−0.11 [-0.27, 0.05]	0.15	0.03 [-0.19, 0.24]	0.93	0.02 [-0.20, 0.23]	0.88
%FEV_1	−0.04 [-0.20, 0.12]	0.6	0.03 [-0.13, 0.19]	0.67	−0.01 [-0.22, 0.21]	0.95	−0.09 [-0.12, 0.30]	0.38
V25/HT	0.18 [0.02, 0.32]	0.024*	0.22 [0.06, 0.37]	0.005**	0.25 [0.04, 0.44]	0.017*	0.24 [0.03, 0.43]	0.023*
Variables	PLA-EX-PA				PLA-ex-PA			
Age	−0.15 [-0.30, 0.01]	0.062	−0.12 [-0.27, 0.04]	0.13	−0.20 [-0.40, 0.01]	0.026*	−0.14 [-0.35, -0.07]	0.18
Height	0.49 [0.30, 0.60]	<0.001**	0.52 [0.39, 0.63]	<0.001**	0.66 [0.53, 0.77]	<0.001**	0.70 [0.57, 0.79]	<0.001**
Weight	0.12 [-0.04, 0.27]	0.14	0.18 [0.02, 0.33]	0.021*	0.22 [0.01, 0.42]	0.036*	0.27 [0.06, 0.45]	0.011*
BMI	−0.29 [-0.42, -0.13]	<0.001**	−0.22 [-0.37, -0.06]	0.005**	−0.30 [-0.48, -0.09]	<0.001**	−0.26 [-0.45, -0.05]	<0.001**
Sex	0.34 [0.20, 0.48]	<0.001**	0.37 [0.23, 0.50]	<0.001**	0.40 [0.21, 0.57]	<0.001**	0.47 [0.29, 0.62]	<0.001**
Pack/ year	0.16 [0.004, 0.31]	0.039*	0.17 [0.01, 0.32]	0.036*	0.09 [-0.12, 0.30]	0.38	0.10 [-0.12, 0.31]	0.35
TV	0.13 [-0.03, 0.28]	0.11	0.12 [-0.04, 0.28]	0.12	0.17 [-0.04, 0.37]	0.1	0.13 [-0.09, 0.33]	0.22
VC	0.42 [0.29, 0.55]	<0.001**	0.48 [0.35, 0.59]	<0.001**	0.59 [0.43, 0.71]	<0.001**	0.63 [0.48, 0.74]	<0.001**
%VC	0.09 [-0.07, 0.24]	0.25	0.13 [-0.02, 0.29]	0.088	0.26 [0.05, 0.44]	0.015*	0.27 [0.06, 0.46]	0.010*
FEV_1	0.40 [0.26, 0.53]	<0.001**	0.45 [0.31, 0.57]	<0.001**	0.54 [0.37, 0.68]	<0.001**	0.58 [0.42, 0.71]	<0.001**
FEV_1%	−0.01 [-0.17. 0.15]	0.94	−0.08 [-0.24, 0.08]	0.3	0.03 [-0.18. 0.25]	0.75	0.01 [-0.20, 0.22]	0.93
%FEV_1	−0.07 [-0.23, 0.09]	0.38	−0.03 [-0.19, 0.12]	0.75	−0.01 [-0.21, 0.22]	0.95	0.08 [-0.14, 0.29]	0.47
V25/HT	0.20 [0.04, 0.35]	0.011*	0.17 [0.02, 0.32]	0.027*	0.26 [0.05, 0.45]	0.012*	0.25 [0.04, 0.44]	0.019*

P values and rank correlation coefficients were calculated using Spearman's correlation. * indicates $P < 0.05$; ** indicates $P < 0.01$; BMI, body mass index; FEV1, forced expiratory volume in one second; FEV1%, forced expiratory volume percent in one second divided by forced vital capacity; %FEV1, percent predicted FEV1; % VC; percent vital capacity; PLA, projected lung area; PLA-INS-PA, PLA of PA view in forced inspiratory phase; PLA-EX-PA, PLA of PA view in forced expiratory phase; PLA-ins-PA, PLA of PA view in tidal inspiratory phase; PLA-ex-PA, PLA of PA view in tidal expiratory phase; TV, tidal volume; V25/ht, the maximum flow rate at 25 % of forced VC divided by body height; VC, vital capacity.

Table 4
Association of PLA of lateral image with each parameter by Spearman's rank correlation.

	Right		Left		Right		Left	
	Spearman's rank correlation coefficient [95 %RI]	P value	Spearman's rank correlation coefficient [95 %RI]	P value	Spearman's rank correlation coefficient [95 %RI]	P value	Spearman's rank correlation coefficient [95 %RI]	P value
Variables	PLA-INS-LAT				PLA-ins-LAT			
Age	0.17 [0.02, 0.32]	0.027*	0.11 [-0.05, 0.26]	0.17	0.23 [0.02, 0.43]	0.026*	0.22 [0.01, 0.42]	0.033*
Height	0.73 [0.65, 0.80]	<0.001**	0.75 [0.67, 0.81]	<0.001**	0.72 [0.59, 0.81]	<0.001**	0.65 [0.51, 0.76]	<0.001**
Weight	0.56 [0.44, 0.66]	<0.001**	0.58 [0.47, 0.68]	<0.001**	0.39 [0.19, 0.55]	<0.001**	0.34 [0.13, 0.51]	0.001**
BMI	0.17 [0.02, 0.32]	0.026*	0.20 [0.04, 0.35]	0.001*	−0.08 [-0.29, 0.14]	0.47	−0.07 [-0.28, 0.14]	0.5
Sex	0.73 [0.64, 0.80]	<0.001**	0.68 [0.59, 0.76]	<0.001**	0.60 [0.44, 0.72]	<0.001**	0.51 [0.33, 0.65]	<0.001**
Pack/ year	0.31 [0.16, 0.44]	<0.001**	0.32 [0.17, 0.45]	<0.001**	0.24 [0.03, 0.43]	0.023*	0.21 [-0.01, 0.40]	0.0504
TV	0.25 [0.10, 0.40]	0.001**	0.21 [0.05, 0.35]	0.008**	0.23 [0.02, 0.42]	0.028*	0.24 [0.03, 0.43]	0.024*
VC	0.65 [0.55, 0.73]	<0.001**	0.70 [0.61, 0.77]	<0.001**	0.48 [0.30, 0.63]	<0.001**	0.45 [0.26, 0.61]	<0.001**
%VC	0.14 [-0.02, 0.30]	0.069	0.22 [0.07, 0.37]	0.005**	0.06 [-0.16, 0.27]	0.58	0.13 [-0.09, 0.33]	0.24
FEV_1	0.54 [0.42, 0.65]	<0.001**	0.59 [0.48, 0.69]	<0.001**	0.37 [0.17, 0.54]	<0.001**	0.34 [0.14, 0.52]	<0.001**
FEV_1%	−0.24 [-0.39.−0.09]	0.002**	−0.21 [-0.36, -0.05]	0.007**	−0.22 [-0.42, -0.01]	0.04*	−0.25 [-0.44, -0.03]	0.02*
%FEV_1	0.02 [-0.14, 0.18]	0.81	0.03 [-0.13, 0.19]	0.69	−0.02 [-0.24, 0.19]	0.83	0.02 [-0.19, 0.23]	0.86
V25/HT	0.08 [-0.08, 0.23]	0.33	0.13 [-0.03, 0.28]	0.11	−0.03 [-0.24, 0.18]	0.76	−0.07 [-0.28, 0.15]	0.51
Variables	PLA-EX-LAT				PLA-ex-LAT			
Age	0.18 [0.03, 0.33]	0.02*	0.13 [-0.03, 0.29]	0.092	0.26 [0.05, 0.45]	0.013*	0.23 [0.02, 0.42]	0.03*
Height	0.54 [0.42, 0.64]	<0.001**	0.57 [0.46, 0.67]	<0.001**	0.67 [0.54, 0.77]	<0.001**	0.62 [0.47, 0.74]	<0.001**
Weight	0.23 [0.08, 0.38]	0.003**	0.30 [0.15, 0.44]	<0.001**	0.29 [0.08, 0.48]	0.005**	0.27 [0.06, 0.45]	0.011*
BMI	−0.11 [-0.27, 0.05]	0.16	−0.04 [-0.20, 0.11]	0.58	−0.18 [-0.38, 0.04]	0.093	−0.15 [-0.35, 0.07]	0.17
Sex	0.54 [0.41, 0.64]	<0.001**	0.50 [0.37, 0.61]	<0.001**	0.55 [0.39, 0.69]	<0.001**	0.48 [0.30, 0.63]	<0.001**
Pack/ year	0.28 [0.13, 0.42]	<0.001**	0.28 [0.13, 0.42]	<0.001**	0.22 [0.009, 0.41]	0.036*	0.17 [-0.05, 0.37]	0.12
TV	0.18 [0.02, 0.33]	0.021*	0.15 [-0.01, 0.30]	0.06	0.15 [-0.06, 0.35]	0.15	0.16 [-0.05, 0.36]	0.12
VC	0.38 [0.24, 0.51]	<0.001**	0.43 [0.30, 0.55]	<0.001**	0.44 [0.25, 0.60]	<0.001**	0.43 [0.23, 0.59]	<0.001**
%VC	−0.05 [-0.21, 0.11]	0.51	0.02 [-0.14, 0.18]	0.78	0.06 [-0.16, 0.27]	0.59	0.11 [-0.11, 0.31]	0.32
FEV_1	0.34 [0.19, 0.48]	<0.001**	0.37 [0.23, 0.50]	<0.001**	0.33 [0.14, 0.52]	<0.001**	0.32 [0.12, 0.50]	0.002**
FEV_1%	−0.13 [-0.29, 0.03]	0.089	−0.14 [-0.29, 0.02]	0.07	−0.20 [-0.40, -0.01]	0.055	0.22 [-0.41, -0.01]	0.036*
%FEV_1	−0.02 [-0.18, 0.14]	0.78	−0.07 [-0.23, 0.09]	0.37	0.03 [-0.19, 0.24]	0.8	0.02 [-0.19, 0.24]	0.82
V25/HT	0.06 [-0.10, 0.21]	0.47	0.06 [-0.10, 0.22]	0.42	−0.04 [-0.25, 0.17]	0.71	−0.07 [-0.28, 0.15]	0.52

P values and rank correlation coefficients were calculated using Spearman's rank correlation. * indicates $P < 0.05$; ** indicates $P < 0.01$; BMI, body mass index; FEV_1, forced expiratory volume in one second; FEV_1%, forced expiratory volume percent in one second divided by forced vital capacity; %FEV_1, percent predicted FEV_1; %VC; percent vital capacity; PLA, projected lung area; PLA-INS-LAT, PLA of lateral view in forced inspiratory phase; PLA-EX-LAT, PLA of lateral view in forced expiratory phase; PLA-ins-LAT, PLA of lateral view in tidal inspiratory phase; PLA-ex-LAT, PLA of lateral view in tidal expiratory phase; TV, tidal volume; V25/ht, the maximum flow rate at 25 % of forced VC divided by body height; VC, vital capacity.

fibrosis of diaphragm muscles [25].

The result of multivariate analysis suggests that BMI, VC and sex can be independent correlation factor. The coefficient of sex in multivariate analysis was higher in lateral views. The PLAs in lateral view is possibly easily subject to the effect of the disproportionate by sex. This can also cause the result that the correlation coefficient with VC and FEV_1 in PA view was higher compared to that with lateral view in univariate analysis.

Our study has several limitations. First, all exams of DXR were performed only at one hospital. Secondly, the influence on the measurement in lateral images by the figure such as curved spines was not assessed, and the error of manual measurement cannot be denied. The outer part of lower lung fields was out of image of PA view in some cases. In lateral image, the border of apical lung fields is often unclear or obscure due to the artifact of bone and soft tissue.

In conclusion, PLA showed statistically significant correlation with pulmonary functions. BMI, sex and VC are independent factors associated with the PLAs. Our results indicate DXR has a possibility to serve as an alternate method for pulmonary function tests in subjects requiring contact inhibition including patients with suspected or confirmed covid-19.

Declaration of competing interest

Dr. Hatabu reports grants from Konica-Minolta Inc, grants from Canon Medical Systems Inc, other from Canon Medical Systems Inc, personal fees from Mitsubishi Chemical Inc, outside the submitted work. The other authors (Takuya Hino, Akinori Hata, Tomoyuki Hida, Yoshitake Yamada, Masako Ueyama, Tetsuro Araki, Takeshi Kamitani, Mizuki Nishino, Atsuko Kurosaki, Masahiro Jinzaki, Kousei Ishigami, Hiroshi Honda, and Shoji Kudoh) have no conflicts of interest to be disclosed related to this article.

Disclosure

Hatabu: Reserch funding from Canon Inc., Canon Medical Systems Inc., and Konica-Minolta Inc.; Consultant to Canon Medical Systems Inc., and Mitsubishi Chemical Co. for outside of writing this manuscript.

CRediT authorship contribution statement

Takuya Hino: Conceptualization, Investigation, Formal analysis, Writing - original draft. **Akinori Hata:** Writing - review & editing. **Tomoyuki Hida:** Writing - review & editing. **Yoshitake Yamada:** Writing - review & editing. **Masako Ueyama:** Data curation, Writing - review & editing. **Tetsuro Araki:** Writing - review & editing. **Takeshi Kamitani:** Writing - review & editing. **Mizuki Nishino:** Writing - review & editing. **Atsuko Kurosaki:** Data curation, Writing - review & editing. **Masahiro Jinzaki:** Writing - review & editing. **Kousei Ishigami:** Writing - review & editing. **Hiroshi Honda:** Writing - review & editing. **Hiroto Hatabu:** Writing - review & editing, Methodology, Project administration, Supervision. **Shoji Kudoh:** Resources, Writing - review & editing.

Table 5
Association of PLA with each parameter by multivariate analysis.

	Right			Left			Right			Left		
	Coefficient	SE	P value	Coefficient	SE	P value	Coefficient	SE	P value	Coefficient	SE	P value
Variables	PLA-INS-PA						PLA-ins-PA					
Intercept	206.9	19.76	<0.001**	149.7	20.69	<0.001**	219	31.54	<0.001**	139	26.91	<0.001**
Age	0.3	0.179	0.0096	0.388	0.188	0.041*	0.162	0.272	0.555	0.513	0.232	0.03
BMI	−3.501	0.537	<0.001**	−3.556	0.565	<0.001**	−4.4	0.814	<0.001**	−4.27	0.694	<0.001**
Sex	8.44	4.543	0.065	4.508	4.778	0.347	6.604	6.984	0.347	1.809	5.958	0.762
VC	26.77	2.428	<0.001**	31.11	3.181	<0.001**	23.48	4.527	<0.001**	29.38	3.862	<0.001**
	PLA-EX-PA						PLA-ex-PA					
Intercept	223.2	25.88	<0.001**	155.6	22.29	<0.001**	209.3	30.39	<0.001**	126.5	24.76	<0.001**
Age	0.026	0.234	0.912	0.181	0.202	0.372	0.19	0.262	0.47	0.512	0.214	0.019*
BMI	−4.636	0.704	<0.001**	−3.801	0.606	<0.001**	−4.753	0.784	<0.001**	−4.001	0.639	<0.001**
Sex	15.15	5.948	0.012*	9.271	5.123	0.072	6.76	6.729	0.318	2.543	5.483	0.644
VC	12.83	3.96	0.0014**	16.31	3.411	<0.001**	23.96	4.362	<0.001**	27.74	3.554	<0.001**
	PLA-INS-LAT						PLA-ins-LAT					
Intercept	139.6	34.94	<0.001**	112.1	34.31	0.0013**	176.7	51.81	<0.001**	160.5	49.12	0.0020**
Age	2.392	0.317	<0.001**	1.98	0.188	<0.001**	2.485	0.447	<0.001**	2.119	0.434	<0.001**
BMI	−2.049	0.95	0.033	−0.867	0.933	0.354	−4.465	1.336	<0.001**	−3.635	1.298	0.0063**
Sex	25.03	4.543	0.0022**	11.36	7.886	0.152	23.47	11.47	0.044*	14.17	11.14	0.207
VC	55.98	5.347	<0.001**	54.8	5.251	<0.001**	41.55	7.436	<0.001**	36.41	7.22	<0.001**
	PLA-EX-LAT						PLA-ex-LAT					
Intercept	266.7	42.28	<0.001**	219.3	38.42	<0.001**	173.2	48.16	<0.001**	155.6	49.12	0.0021**
Age	1.269	0.383	0.0011**	0.908	0.348	0.00996**	2.645	0.416	<0.001**	2.141	0.424	<0.001**
BMI	−6.154	1.15	<0.001**	−3.47	1.045	0.0011**	−6.583	1.242	<0.001**	−4.857	1.267	0.0011**
Sex	42.28	9.72	<0.001**	28.86	8.831	0.0013**	22.31	10.66	0.039*	12.12	10.88	0.268
VC	18.02	6.471	0.0060**	17.66	5.88	0.0031**	43.2	6.913	<0.001**	37.25	7.05	<0.001**

Coefficient, standard error (SE), and P values were calculated using multiple linear regression analysis. * indicates $P < 0.05$; ** indicates $P < 0.01$; BMI, body mass index; PLA, projected lung area; PLA-INS-PA, PLA of PA view in forced inspiratory phase; PLA-EX-PA, PLA of PA view in forced expiratory phase; PLA-INS-LAT, PLA of lateral view in forced inspiratory phase; PLA-EX-LAT, PLA of lateral view in forced expiratory phase; PLA-ins-PA, PLA of PA view in tidal inspiratory phase; PLA-ex-PA, PLA of PA view in tidal expiratory phase; PLA-ins-LAT, PLA of lateral view in tidal inspiratory phase; PLA-ex-LAT, PLA of lateral view in tidal expiratory phase; VC, vital capacity.

Acknowledgements

Grant information: The investigator, HH is supported by R01CA203636 and U01CA209414 (NCI).

References

[1] C.J. Zappala, P.I. Latsi, A.G. Nicholson, T.V. Colby, D. Cramer, E.A. Renzoni, D. M. Hansell, R.M. du Bois, A.U. Wells, Marginal decline in forced vital capacity is associated with a poor outcome in idiopathic pulmonary fibrosis, Eur. Respir. J. 35 (2010) 830–836, https://doi.org/10.1183/09031936.00155108.

[2] C.F. Vogelmeier, G.J. Criner, F.J. Martínez, A. Anzueto, P.J. Barnes, J. Bourbeau, B. R. Celli, R. Chen, M. Decramer, L.M. Fabbri, P. Frith, D.M.G. Halpin, M.V. López Varela, M. Nishimura, N. Roche, R. Rodríguez-Roisin, D.D. Sin, D. Singh, R. Stockley, J. Vestbo, J.A. Wedzicha, A. Agustí, Global strategy for the diagnosis, management, and prevention of chronic obstructive lung disease 2017 Report: GOLD Executive Summary, Respirology 22 (2017) 575–601, https://doi.org/10.1016/j.arbres.2017.02.001.

[3] S. Mirza, R.D. Clay, M.A. Koslow, P.D. Scanlon, COPD Guidelines: A Review of the 2018 GOLD Report, Mayo Clin. Proc. 93 (2018) 1488–1502, https://doi.org/10.1016/j.mayocp.2018.05.026.

[4] G. Raghu, M. Remy-Jardin, J.L. Myers, L. Richeldi, C.J. Ryerson, D.J. Lederer, J. Behr, V. Cottin, S.K. Danoff, F. Morell, K.R. Flaherty, A. Wells, F.J. Martinez, A. Azuma, T.J. Bice, D. Bouros, K.K. Brown, H.R. Collard, A. Duggal, L. Galvin, Y. Inoue, R.G. Jenkins, T. Johkoh, E.A. Kazerooni, M. Kitaichi, S.L. Knight, G. Mansour, A.G. Nicholson, S.N.J. Pipavath, I. Buendía-Roldán, M. Selman, W. D. Travis, S. Walsh, K.C. Wilson, American thoracic society, european respiratory society, japanese respiratory society, and latin american thoracic society, diagnosis of idiopathic pulmonary fibrosis. An Official ATS/ERS/JRS/ALAT Clinical Practice Guideline, Am. J. Respir. Crit. Care Med. 198 (2018) e44–e68, https://doi.org/10.1164/rccm.201807-1255ST.

[5] H.J. Barnhard, J.A. Pierce, J.W. Joyce, J.H. Bates, Roentgenographic determination of total lung capacity. A new method evaluated in health, emphysema and congestive heart failure, Am. J. Med. 28 (1960) 51–60, https://doi.org/10.1016/0002-9343(60)90222-9.

[6] H.M. Loyd, T. String, A.B. DuBois, Radiographic and plethysmographic determination of total lung capacity, Radiology 86 (1966) 7–14, https://doi.org/10.1148/86.1.7.

[7] P.C. Pratt, G.A. Klugh, A method for the determination of total lung capacity from posteroanterior and lateral chest roentgenograms, Am. Rev. Respir. Dis. 96 (1967) 548–552, https://doi.org/10.1164/arrd.1967.96.3.548.

[8] T.R. Harris, P.C. Pratt, K.H. Kilburn, Total lung capacity measured by roentgenograms, Am. J. Med. 50 (1971) 756–763, https://doi.org/10.1016/0002-9343(71)90183-5.

[9] G. Gamsu, D.M. Shames, J. McMahon, R.H. Greenspan, Radiographically determined lung volumes at full inspiration and during dynamic forced expiration in normal subjects, Invest. Radiol. 10 (1975) 100–108, https://doi.org/10.1097/00004424-197503000-00002.

[10] R.J. Pierce, D.J. Brown, M. Holmes, D.M. Denison, Estimation of lung volumes from chest radiographs using shape information, Thorax 34 (1979) 726–734, https://doi.org/10.1136/thx.34.6.726.

[11] A.E. Schlesinger, D.K. White, G.B. Mallory, C.F. Hildeboldt, C.B. Huddleston, Estimation of total lung capacity from chest radiography and chest CT in children: comparison with body plethysmography, Am. J. Roentgenol. 165 (1995) 151–154, https://doi.org/10.2214/ajr.165.1.7785574.

[12] J. Clausen, Measurement of absolute lung volumes by imaging techniques, Eur. Respir. J. 10 (1997) 2427–2431, https://doi.org/10.1183/09031936.97.10102427.

[13] C.H. Park, S.J. Haam, S. Lee, K.H. Han, T.H. Kim, Prediction of anatomical lung volume using planimetric measurements on chest radiographs, Acta radiol. 57 (2016) 1066–1071, https://doi.org/10.1177/0284185115618548.

[14] R. Tanaka, Dynamic chest radiography: flat-panel detector (FPD) based functional X-ray imaging, Radiol. Phys. Technol. 9 (2016) 139–153, https://doi.org/10.1007/s12194-016-0361-6.

[15] R. Tanaka, S. Sanada, N. Okazaki, T. Kobayashi, M. Fujimura, M. Yasui, T. Matsui, K. Nakayama, Y. Nanbu, O. Matsui, Evaluation of pulmonary function using breathing chest radiography with a dynamic flat-panel detector (FPD): primary results in pulmonary diseases, Invest. Radiol. 41 (2016) 735–745, https://doi.org/10.1097/01.rli.0000236904.79265.68.

[16] Y. Yamada, M. Ueyama, T. Abe, T. Araki, T. Abe, M. Nishino, M. Jinzaki, H. Hatabu, S. Kudoh, Time-resolved quantitative analysis of the diaphragms during tidal breathing in a standing position using dynamic chest radiography with a flat panel detector system ("Dynamic X-Ray phrenicography"): initial experience in 172 volunteers, Acad. Radiol. 24 (2017) 393–400, https://doi.org/10.1016/j.acra.2016.11.014.

[17] Y. Yamada, M. Ueyama, T. Abe, T. Araki, T. Abe, M. Nishino, M. Jinzaki, H. Hatabu, S. Kudoh, Difference in diaphragmatic motion during tidal breathing in a standing position between COPD patients and normal subjects: time-resolved quantitative evaluation using dynamic chest radiography with flat panel detector system ("dynamic X-ray phrenicography"), Eur. J. Radiol. 87 (2017) 76–82, https://doi.org/10.1016/j.ejrad.2016.12.014.

[18] T. Hida, Y. Yamada, M. Ueyama, T. Araki, M. Nishino, A. Kurosaki, M. Jinzaki, H. Honda, H. Hatabu, S. Kudoh, Time-resolved quantitative evaluation of diaphragmatic motion during forced breathing in a health screening cohort in a standing position: dynamic chest phrenicography, Eur. J. Radiol. 113 (2019) 59–65, https://doi.org/10.1016/j.ejrad.2019.01.034.

[19] T. Hida, Y. Yamada, M. Ueyama, T. Araki, M. Nishino, A. Kurosaki, M. Jinzaki, H. Honda, H. Hatabu, S. Kudoh, Decreased and slower diaphragmatic motion during forced breathing in severe COPD patients: time-resolved quantitative

analysis using dynamic chest radiography with a flat panel detector system, Eur. J. Radiol. 112 (2019) 28–36, https://doi.org/10.1016/j.ejrad.2018.12.023.
[20] Y. Yamada, M. Ueyama, T. Abe, T. Araki, T. Abe, M. Nishino, M. Jinzaki, H. Hatabu, S. Kudoh, Difference in the craniocaudal gradient of the maximum pixel value change rate between chronic obstructive pulmonary disease patients and normal subjects using sub-mGy dynamic chest radiography with a flat panel detector system, Eur. J. Radiol. 92 (2017) 37–44, https://doi.org/10.1016/j.ejrad.2017.04.016.
[21] B.L. Graham, I. Steenbruggen, M.R. Miller, I.Z. Barjaktarevic, B.G. Cooper, G. L. Hall, T.S. Hallstrand, D.A. Kaminsky, K. McCarthy, M.C. McCormack, C. E. Oropez, M. Rosenfeld, S. Stanojevic, M.P. Swanney, B.R. Thompson, Standardization of spirometry 2019 update. An official american thoracic society and european respiratory society technical statement, Am. J. Respir. Crit. Care Med. 200 (2019) e70–e88, https://doi.org/10.1164/rccm.201908-1590ST.
[22] Y. Kanda, Investigation of the freely available easy-to-use software' EZR' for medical statistics, Bone Marrow Transplant. 48 (2013) 452–458, https://doi.org/10.1038/bmt.2012.244.
[23] R Core Team, R, A Language and Environment for Statistical Computing, Vienna: R Foundation for Statistical Computing, 2019.
[24] H.G. Chotas, C.E. Ravin, Chest radiography: estimated lung volume and projected area obscured by the heart, mediastinum, and diaphragm, Radiology 193 (1994), https://doi.org/10.1148/radiology.193.2.7972752, 403-404. 1.
[25] R.A.B. Nucci, R.R. de Souza, C.K. Suemoto, A.L. Busse, L.B.M. Maifrino, C. A. Pasqualucci, C.A. Anaruma, W. Jacob-Filho, Cigarette smoking impairs the diaphragm muscle structure of patients without respiratory pathologies: an autopsy study, Cell. Physiol. Biochem. 53 (2019) 648–655, https://doi.org/10.33594/000000163.